Search for $Z' \to e^+e^-$ Using Dielectron Mass and Angular Distribution

A. Abulencia,[23] D. Acosta,[17] J. Adelman,[13] T. Affolder,[10] T. Akimoto,[55] M.G. Albrow,[16] D. Ambrose,[16] S. Amerio,[43] D. Amidei,[34] A. Anastassov,[52] K. Anikeev,[16] A. Annovi,[18] J. Antos,[1] M. Aoki,[55] G. Apollinari,[16] J.-F. Arguin,[33] T. Arisawa,[57] A. Artikov,[14] W. Ashmanskas,[16] A. Attal,[8] F. Azfar,[42] P. Azzi-Bacchetta,[43] P. Azzurri,[46] N. Bacchetta,[43] H. Bachacou,[28] W. Badgett,[16] A. Barbaro-Galtieri,[28] V.E. Barnes,[48] B.A. Barnett,[24] S. Baroiant,[7] V. Bartsch,[30] G. Bauer,[32] F. Bedeschi,[46] S. Behari,[24] S. Belforte,[54] G. Bellettini,[46] J. Bellinger,[59] A. Belloni,[32] E. Ben Haim,[44] D. Benjamin,[15] A. Beretvas,[16] J. Beringer,[28] T. Berry,[29] A. Bhatti,[50] M. Binkley,[16] D. Bisello,[43] R. E. Blair,[2] C. Blocker,[6] B. Blumenfeld,[24] A. Bocci,[15] A. Bodek,[49] V. Boisvert,[49] G. Bolla,[48] A. Bolshov,[32] D. Bortoletto,[48] J. Boudreau,[47] A. Boveia,[10] B. Brau,[10] C. Bromberg,[35] E. Brubaker,[13] J. Budagov,[14] H.S. Budd,[49] S. Budd,[23] K. Burkett,[16] G. Busetto,[43] P. Bussey,[20] K. L. Byrum,[2] S. Cabrera,[15] M. Campanelli,[19] M. Campbell,[34] F. Canelli,[8] A. Canepa,[48] D. Carlsmith,[59] R. Carosi,[46] S. Carron,[15] M. Casarsa,[54] A. Castro,[5] P. Catastini,[46] D. Cauz,[54] M. Cavalli-Sforza,[3] A. Cerri,[28] L. Cerrito,[42] S.H. Chang,[27] J. Chapman,[34] Y.C. Chen,[1] M. Chertok,[7] G. Chiarelli,[46] G. Chlachidze,[14] F. Chlebana,[16] I. Cho,[27] K. Cho,[27] D. Chokheli,[14] J.P. Chou,[21] P.H. Chu,[23] S.H. Chuang,[59] K. Chung,[12] W.H. Chung,[59] Y.S. Chung,[49] M. Ciljak,[46] C.I. Ciobanu,[23] M.A. Ciocci,[46] A. Clark,[19] D. Clark,[6] M. Coca,[15] G. Compostella,[43] M.E. Convery,[50] J. Conway,[7] B. Cooper,[30] K. Copic,[34] M. Cordelli,[18] G. Cortiana,[43] F. Cresciolo,[46] A. Cruz,[17] C. Cuenca Almenar,[7] J. Cuevas,[11] R. Culbertson,[16] D. Cyr,[59] S. DaRonco,[43] S. D'Auria,[20] M. D'Onofrio,[3] D. Dagenhart,[6] P. de Barbaro,[49] S. De Cecco,[51] A. Deisher,[28] G. De Lentdecker,[49] M. Dell'Orso,[46] F. Delli Paoli,[43] S. Demers,[49] L. Demortier,[50] J. Deng,[15] M. Deninno,[5] D. De Pedis,[51] P.F. Derwent,[16] C. Dionisi,[51] J.R. Dittmann,[4] P. DiTuro,[52] C. Dörr,[25] S. Donati,[46] M. Donega,[19] P. Dong,[8] J. Donini,[43] T. Dorigo,[43] S. Dube,[52] K. Ebina,[57] J. Efron,[39] J. Ehlers,[19] R. Erbacher,[7] D. Errede,[23] S. Errede,[23] R. Eusebi,[16] H.C. Fang,[28] S. Farrington,[29] I. Fedorko,[46] W.T. Fedorko,[13] R.G. Feild,[60] M. Feindt,[25] J.P. Fernandez,[31] R. Field,[17] G. Flanagan,[48] L.R. Flores-Castillo,[47] A. Foland,[21] S. Forrester,[7] G.W. Foster,[16] M. Franklin,[21] J.C. Freeman,[28] I. Furic,[13] M. Gallinaro,[50] J. Galyardt,[12] J.E. Garcia,[46] M. Garcia Sciveres,[28] A.F. Garfinkel,[48] C. Gay,[60] H. Gerberich,[23] D. Gerdes,[34] S. Giagu,[51] P. Giannetti,[46] A. Gibson,[28] K. Gibson,[12] C. Ginsburg,[16] N. Giokaris,[14] K. Giolo,[48] M. Giordani,[54] P. Giromini,[18] M. Giunta,[46] G. Giurgiu,[12] V. Glagolev,[14] D. Glenzinski,[16] M. Gold,[37] N. Goldschmidt,[34] J. Goldstein,[42] G. Gomez,[11] G. Gomez-Ceballos,[11] M. Goncharov,[53] O. González,[31] I. Gorelov,[37] A.T. Goshaw,[15] Y. Gotra,[47] K. Goulianos,[50] A. Gresele,[43] M. Griffiths,[29] S. Grinstein,[21] C. Grosso-Pilcher,[13] R.C. Group,[17] U. Grundler,[23] J. Guimaraes da Costa,[21] Z. Gunay-Unalan,[35] C. Haber,[28] S.R. Hahn,[16] K. Hahn,[45] E. Halkiadakis,[52] A. Hamilton,[33] B.-Y. Han,[49] J.Y. Han,[49] R. Handler,[59] F. Happacher,[18] K. Hara,[55] M. Hare,[56] S. Harper,[42] R.F. Harr,[58] R.M. Harris,[16] K. Hatakeyama,[50] J. Hauser,[8] C. Hays,[15] A. Heijboer,[45] B. Heinemann,[29] J. Heinrich,[45] M. Herndon,[59] D. Hidas,[15] C.S. Hill,[10] D. Hirschbuehl,[25] A. Hocker,[16] A. Holloway,[21] S. Hou,[1] M. Houlden,[29] S.-C. Hsu,[9] B.T. Huffman,[42] R.E. Hughes,[39] J. Huston,[35] J. Incandela,[10] G. Introzzi,[46] M. Iori,[51] Y. Ishizawa,[55] A. Ivanov,[7] B. Iyutin,[32] E. James,[16] D. Jang,[52] B. Jayatilaka,[34] D. Jeans,[51] H. Jensen,[16] E.J. Jeon,[27] S. Jindariani,[17] M. Jones,[48] K.K. Joo,[27] S.Y. Jun,[12] T.R. Junk,[23] T. Kamon,[53] J. Kang,[34] P.E. Karchin,[58] Y. Kato,[41] Y. Kemp,[25] R. Kephart,[16] U. Kerzel,[25] V. Khotilovich,[53] B. Kilminster,[39] D.H. Kim,[27] H.S. Kim,[27] J.E. Kim,[27] M.J. Kim,[12] S.B. Kim,[27] S.H. Kim,[55] Y.K. Kim,[13] L. Kirsch,[6] S. Klimenko,[17] M. Klute,[32] B. Knuteson,[32] B.R. Ko,[15] H. Kobayashi,[55] K. Kondo,[57] D.J. Kong,[27] J. Konigsberg,[17] A. Korytov,[17] A.V. Kotwal,[15] A. Kovalev,[45] A. Kraan,[45] J. Kraus,[23] I. Kravchenko,[32] M. Kreps,[25] J. Kroll,[45] N. Krumnack,[4] M. Kruse,[15] V. Krutelyov,[53] S. E. Kuhlmann,[2] Y. Kusakabe,[57] S. Kwang,[13] A.T. Laasanen,[48] S. Lai,[33] S. Lami,[46] S. Lammel,[16] M. Lancaster,[30] R.L. Lander,[7] K. Lannon,[39] A. Lath,[52] G. Latino,[46] I. Lazzizzera,[43] T. LeCompte,[2] J. Lee,[49] J. Lee,[27] Y.J. Lee,[27] S.W. Lee,[53] R. Lefèvre,[3] N. Leonardo,[32] S. Leone,[46] S. Levy,[13] J.D. Lewis,[16] C. Lin,[60] C.S. Lin,[16] M. Lindgren,[16] E. Lipeles,[9] T.M. Liss,[23] A. Lister,[19] D.O. Litvintsev,[16] T. Liu,[16] N.S. Lockyer,[45] A. Loginov,[36] M. Loreti,[43] P. Loverre,[51] R.-S. Lu,[1] D. Lucchesi,[43] P. Lujan,[28] P. Lukens,[16] G. Lungu,[17] L. Lyons,[42] J. Lys,[28] R. Lysak,[1] E. Lytken,[48] P. Mack,[25] D. MacQueen,[33] R. Madrak,[16] K. Maeshima,[16] T. Maki,[22] P. Maksimovic,[24] S. Malde,[42] G. Manca,[29] F. Margaroli,[5] R. Marginean,[16] C. Marino,[23] A. Martin,[60] V. Martin,[38] M. Martínez,[3] T. Maruyama,[55] H. Matsunaga,[55] M.E. Mattson,[58] R. Mazini,[33] P. Mazzanti,[5] K.S. McFarland,[49] P. McIntyre,[53] R. McNulty,[29] A. Mehta,[29] S. Menzemer,[11] A. Menzione,[46] P. Merkel,[48] C. Mesropian,[50] A. Messina,[51] M. von der Mey,[8] T. Miao,[16] N. Miladinovic,[6] J. Miles,[32] R. Miller,[35] J.S. Miller,[34] C. Mills,[10] M. Milnik,[25] R. Miquel,[28] A. Mitra,[1] G. Mitselmakher,[17] A. Miyamoto,[26] N. Moggi,[5] B. Mohr,[8] R. Moore,[16]

M. Morello,[46] P. Movilla Fernandez,[28] J. Mülmenstädt,[28] A. Mukherjee,[16] Th. Muller,[25] R. Mumford,[24] P. Murat,[16] J. Nachtman,[16] J. Naganoma,[57] S. Nahn,[32] I. Nakano,[40] A. Napier,[56] D. Naumov,[37] V. Necula,[17] C. Neu,[45] M.S. Neubauer,[9] J. Nielsen,[28] T. Nigmanov,[47] L. Nodulman,[2] O. Norniella,[3] E. Nurse,[30] T. Ogawa,[57] S.H. Oh,[15] Y.D. Oh,[27] T. Okusawa,[41] R. Oldeman,[29] R. Orava,[22] K. Osterberg,[22] C. Pagliarone,[46] E. Palencia,[11] R. Paoletti,[46] V. Papadimitriou,[16] A.A. Paramonov,[13] B. Parks,[39] S. Pashapour,[33] J. Patrick,[16] G. Pauletta,[54] M. Paulini,[12] C. Paus,[32] D.E. Pellett,[7] A. Penzo,[54] T.J. Phillips,[15] G. Piacentino,[46] J. Piedra,[44] L. Pinera,[17] K. Pitts,[23] C. Plager,[8] L. Pondrom,[59] X. Portell,[3] O. Poukhov,[14] N. Pounder,[42] F. Prakoshyn,[14] A. Pronko,[16] J. Proudfoot,[2] F. Ptohos,[18] G. Punzi,[46] J. Pursley,[24] J. Rademacker,[42] A. Rahaman,[47] A. Rakitin,[32] S. Rappoccio,[21] F. Ratnikov,[52] B. Reisert,[16] V. Rekovic,[37] N. van Remortel,[22] P. Renton,[42] M. Rescigno,[51] S. Richter,[25] F. Rimondi,[5] L. Ristori,[46] W.J. Robertson,[15] A. Robson,[20] T. Rodrigo,[11] E. Rogers,[23] S. Rolli,[56] R. Roser,[16] M. Rossi,[54] R. Rossin,[17] C. Rott,[48] A. Ruiz,[11] J. Russ,[12] V. Rusu,[13] H. Saarikko,[22] S. Sabik,[33] A. Safonov,[53] W.K. Sakumoto,[49] G. Salamanna,[51] O. Saltó,[3] D. Saltzberg,[8] C. Sanchez,[3] L. Santi,[54] S. Sarkar,[51] L. Sartori,[46] K. Sato,[55] P. Savard,[33] A. Savoy-Navarro,[44] T. Scheidle,[25] P. Schlabach,[16] E.E. Schmidt,[16] M.P. Schmidt,[60] M. Schmitt,[38] T. Schwarz,[34] L. Scodellaro,[11] A.L. Scott,[10] A. Scribano,[46] F. Scuri,[46] A. Sedov,[48] S. Seidel,[37] Y. Seiya,[41] A. Semenov,[14] L. Sexton-Kennedy,[16] I. Sfiligoi,[18] M.D. Shapiro,[28] T. Shears,[29] P.F. Shepard,[47] D. Sherman,[21] M. Shimojima,[55] M. Shochet,[13] Y. Shon,[59] I. Shreyber,[36] A. Sidoti,[44] P. Sinervo,[33] A. Sisakyan,[14] J. Sjolin,[42] A. Skiba,[25] A.J. Slaughter,[16] K. Sliwa,[56] J.R. Smith,[7] F.D. Snider,[16] R. Snihur,[33] M. Soderberg,[34] A. Soha,[7] S. Somalwar,[52] V. Sorin,[35] J. Spalding,[16] M. Spezziga,[16] F. Spinella,[46] T. Spreitzer,[33] P. Squillacioti,[46] M. Stanitzki,[60] A. Staveris-Polykalas,[46] R. St. Denis,[20] B. Stelzer,[8] O. Stelzer-Chilton,[42] D. Stentz,[38] J. Strologas,[37] D. Stuart,[10] J.S. Suh,[27] A. Sukhanov,[17] K. Sumorok,[32] H. Sun,[56] T. Suzuki,[55] A. Taffard,[23] R. Takashima,[40] Y. Takeuchi,[55] K. Takikawa,[55] M. Tanaka,[2] R. Tanaka,[40] N. Tanimoto,[40] M. Tecchio,[34] P.K. Teng,[1] K. Terashi,[50] S. Tether,[32] J. Thom,[16] A.S. Thompson,[20] E. Thomson,[45] P. Tipton,[49] V. Tiwari,[12] S. Tkaczyk,[16] D. Toback,[53] S. Tokar,[14] K. Tollefson,[35] T. Tomura,[55] D. Tonelli,[46] M. Tönnesmann,[35] S. Torre,[18] D. Torretta,[16] S. Tourneur,[44] W. Trischuk,[33] R. Tsuchiya,[57] S. Tsuno,[40] N. Turini,[46] F. Ukegawa,[55] T. Unverhau,[20] S. Uozumi,[55] D. Usynin,[45] A. Vaiciulis,[49] S. Vallecorsa,[19] A. Varganov,[34] E. Vataga,[37] G. Velev,[16] G. Veramendi,[23] V. Veszpremi,[48] R. Vidal,[16] I. Vila,[11] R. Vilar,[11] T. Vine,[30] I. Vollrath,[33] I. Volobouev,[28] G. Volpi,[46] F. Würthwein,[9] P. Wagner,[53] R. G. Wagner,[2] R.L. Wagner,[16] W. Wagner,[25] R. Wallny,[8] T. Walter,[25] Z. Wan,[52] S.M. Wang,[1] A. Warburton,[33] S. Waschke,[20] D. Waters,[30] W.C. Wester III,[16] B. Whitehouse,[56] D. Whiteson,[45] A.B. Wicklund,[2] E. Wicklund,[16] G. Williams,[33] H.H. Williams,[45] P. Wilson,[16] B.L. Winer,[39] P. Wittich,[16] S. Wolbers,[16] C. Wolfe,[13] T. Wright,[34] X. Wu,[19] S.M. Wynne,[29] A. Yagil,[16] K. Yamamoto,[41] J. Yamaoka,[52] T. Yamashita,[40] C. Yang,[60] U.K. Yang,[13] Y.C. Yang,[27] W.M. Yao,[28] G.P. Yeh,[16] J. Yoh,[16] K. Yorita,[13] T. Yoshida,[41] G.B. Yu,[49] I. Yu,[27] S.S. Yu,[16] J.C. Yun,[16] L. Zanello,[51] A. Zanetti,[54] I. Zaw,[21] F. Zetti,[46] X. Zhang,[23] J. Zhou,[52] and S. Zucchelli[5]

(CDF Collaboration)

[1]*Institute of Physics, Academia Sinica, Taipei, Taiwan 11529, Republic of China*
[2]*Argonne National Laboratory, Argonne, Illinois 60439*
[3]*Institut de Fisica d'Altes Energies, Universitat Autonoma de Barcelona, E-08193, Bellaterra (Barcelona), Spain*
[4]*Baylor University, Waco, Texas 76798*
[5]*Istituto Nazionale di Fisica Nucleare, University of Bologna, I-40127 Bologna, Italy*
[6]*Brandeis University, Waltham, Massachusetts 02254*
[7]*University of California, Davis, Davis, California 95616*
[8]*University of California, Los Angeles, Los Angeles, California 90024*
[9]*University of California, San Diego, La Jolla, California 92093*
[10]*University of California, Santa Barbara, Santa Barbara, California 93106*
[11]*Instituto de Fisica de Cantabria, CSIC-University of Cantabria, 39005 Santander, Spain*
[12]*Carnegie Mellon University, Pittsburgh, PA 15213*
[13]*Enrico Fermi Institute, University of Chicago, Chicago, Illinois 60637*
[14]*Joint Institute for Nuclear Research, RU-141980 Dubna, Russia*
[15]*Duke University, Durham, North Carolina 27708*
[16]*Fermi National Accelerator Laboratory, Batavia, Illinois 60510*
[17]*University of Florida, Gainesville, Florida 32611*
[18]*Laboratori Nazionali di Frascati, Istituto Nazionale di Fisica Nucleare, I-00044 Frascati, Italy*
[19]*University of Geneva, CH-1211 Geneva 4, Switzerland*
[20]*Glasgow University, Glasgow G12 8QQ, United Kingdom*
[21]*Harvard University, Cambridge, Massachusetts 02138*

[22] Division of High Energy Physics, Department of Physics,
University of Helsinki and Helsinki Institute of Physics, FIN-00014, Helsinki, Finland
[23] University of Illinois, Urbana, Illinois 61801
[24] The Johns Hopkins University, Baltimore, Maryland 21218
[25] Institut für Experimentelle Kernphysik, Universität Karlsruhe, 76128 Karlsruhe, Germany
[26] High Energy Accelerator Research Organization (KEK), Tsukuba, Ibaraki 305, Japan
[27] Center for High Energy Physics: Kyungpook National University, Taegu 702-701; Seoul National University,
Seoul 151-742; and SungKyunKwan University, Suwon 440-746; Korea
[28] Ernest Orlando Lawrence Berkeley National Laboratory, Berkeley, California 94720
[29] University of Liverpool, Liverpool L69 7ZE, United Kingdom
[30] University College London, London WC1E 6BT, United Kingdom
[31] Centro de Investigaciones Energeticas Medioambientales y Tecnologicas, E-28040 Madrid, Spain
[32] Massachusetts Institute of Technology, Cambridge, Massachusetts 02139
[33] Institute of Particle Physics: McGill University, Montréal,
Canada H3A 2T8; and University of Toronto, Toronto, Canada M5S 1A7
[34] University of Michigan, Ann Arbor, Michigan 48109
[35] Michigan State University, East Lansing, Michigan 48824
[36] Institution for Theoretical and Experimental Physics, ITEP, Moscow 117259, Russia
[37] University of New Mexico, Albuquerque, New Mexico 87131
[38] Northwestern University, Evanston, Illinois 60208
[39] The Ohio State University, Columbus, Ohio 43210
[40] Okayama University, Okayama 700-8530, Japan
[41] Osaka City University, Osaka 588, Japan
[42] University of Oxford, Oxford OX1 3RH, United Kingdom
[43] University of Padova, Istituto Nazionale di Fisica Nucleare,
Sezione di Padova-Trento, I-35131 Padova, Italy
[44] LPNHE-Universite Pierre et Marie Curie-Paris 6, UMR7585, Paris F-75005 France; IN2P3-CNRS
[45] University of Pennsylvania, Philadelphia, Pennsylvania 19104
[46] Istituto Nazionale di Fisica Nucleare Pisa, Universities of Pisa,
Siena and Scuola Normale Superiore, I-56127 Pisa, Italy
[47] University of Pittsburgh, Pittsburgh, Pennsylvania 15260
[48] Purdue University, West Lafayette, Indiana 47907
[49] University of Rochester, Rochester, New York 14627
[50] The Rockefeller University, New York, New York 10021
[51] Istituto Nazionale di Fisica Nucleare, Sezione di Roma 1,
University of Rome "La Sapienza," I-00185 Roma, Italy
[52] Rutgers University, Piscataway, New Jersey 08855
[53] Texas A&M University, College Station, Texas 77843
[54] Istituto Nazionale di Fisica Nucleare, University of Trieste/ Udine, Italy
[55] University of Tsukuba, Tsukuba, Ibaraki 305, Japan
[56] Tufts University, Medford, Massachusetts 02155
[57] Waseda University, Tokyo 169, Japan
[58] Wayne State University, Detroit, Michigan 48201
[59] University of Wisconsin, Madison, Wisconsin 53706
[60] Yale University, New Haven, Connecticut 06520

We search for Z' bosons in dielectron events produced in $p\bar{p}$ collisions at $\sqrt{s} = 1.96$ TeV, using a 0.45 fb^{-1} dataset accumulated with the CDF II detector at the Fermilab Tevatron. To identify the $Z' \to e^+e^-$ signal, both the dielectron invariant mass distribution and the angular distribution of the electron pair are used. No evidence of a signal is found, and 95% confidence level lower limits are set on the Z' mass for several models. Limits are also placed on the mass and gauge coupling of a generic Z', as well as on the contact interaction mass scales for different helicity structure scenarios.

PACS numbers: 13.85.Rm, 13.85.Qk, 14.70.Pw, 12.60.Cn

Many extensions of the standard model (SM) gauge group predict the existence of electrically-neutral, massive gauge bosons commonly referred to as Z' [1, 2, 3, 4, 5]. The leptonic decays $Z' \to \ell^+\ell^-$ provide the most distinctive signature for observing the Z' signal at a hadron collider. In two recent publications, the Collider Detector at Fermilab (CDF) Collaboration has set limits on different Z' models by analyzing the invariant mass ($M_{\ell\ell}$) spectrum of the dielectron, dimuon, and ditau final states, using a dataset corresponding to an integrated luminosity of approximately 0.2 fb^{-1} [6, 7]. Besides the dilepton mass $M_{\ell\ell}$, it has been shown that the angular distribution of the dilepton events can also be used to test the presence of a Z' boson by detecting its in-

terference with the SM Z boson [8]. In this Letter, for the first time at a hadron collider, the massive resonance search technique ($M_{\ell\ell}$ analysis) is extended to include dilepton angular information to detect $Z' \to e^+e^-$ decays in 0.45 fb^{-1} of data accumulated with the CDF II detector. As the integrated luminosity increases, the sensitivity of the standard $M_{\ell\ell}$ analysis plateaus; adding the angular information starts to become an important handle for extending the Z' exclusion reach and discovery potential. In this Letter many of the theoretical Z' models are surveyed, and results are reported for the sequential Z'_{SM}, the canonical superstring-inspired E_6 models Z_χ, Z_ψ, Z_η, Z_I, Z_N, $Z_{\rm sec}$ [9, 10], the "littlest" Higgs Z_H model [4, 5], the four generic model-lines of Ref. [2], and contact-interaction searches. No significant evidence of a Z' signal is found, and the tightest constraints to date are set on most of these models.

The CDF detector is described in detail elsewhere [11]. For this study, the relevant subdetector systems are the central tracking chamber (COT) and the central and the plug calorimeters. The COT is a 96-layer open-cell drift chamber immersed in a 1.4 Tesla magnetic field, used to measure charged particle momenta within the pseudorapidity range $|\eta| < 1.0$ [12]. Surrounding the COT are the electromagnetic (EM) and hadronic (HAD) calorimeters, segmented in projective $\eta - \phi$ towers pointing to the nominal collision point $z = 0$. The central calorimeters measure the energies of particles within the range $|\eta| < 1.1$, while the plug calorimeters extend the range to $1.1 < |\eta| < 3.6$. Two triggers were used to select the data for this analysis. The main trigger requires two high-E_T EM clusters in the calorimeter while a backup trigger accepts events with a single electron candidate with very high E_T and looser electron-selection requirements.

Events are selected with two high-E_T electron candidates [13, 14], of which at least one is required to have been measured in the central calorimeter. A matching COT track is required for all central candidates. Events with same-sign central electron pairs are rejected, and an isolation condition for the energy found within a cone of angular radius $R = \sqrt{(\Delta\eta)^2 + (\Delta\phi)^2} = 0.4$ around the electron is imposed for electron candidates. The angular distribution is measured using $\cos\theta^*$, where θ^* is the angle between the electron and the incoming quark in the Collins-Soper frame [15]. The search is performed using events with $M_{ee} > 200$ GeV/c^2.

Z' production is expected to interfere with the SM Drell-Yan Z/γ^* process, altering the $\cos\theta^*$ distribution. For this reason, the Z/γ^* process is not labeled as a "background". Instead, the $Z'/Z/\gamma^*$ is referred to as the Z' *signal*, while the SM Z/γ^* is referred to as the *SM Drell-Yan* production. The term *background* will be used to designate all other SM processes (excluding Z/γ^*) expected to contribute to the dielectron final state sample. Of these background sources, the most important are dijet events in which jets are misidentified as electrons, and diboson events (see Table I). The dijet background is estimated using the probability for a jet to be misidentified as an electron ("fake rate") which is measured in inclusive jet triggered data. The fake rate is then applied to each jet in a sample of events containing one electron candidate and one or more jets. All non-dijet backgrounds are estimated using PYTHIA [16] Monte Carlo simulation, normalized to the product of the theoretical cross sections [17, 18] and the integrated luminosity. Other background processes such as $Z/\gamma^* \to \tau^+\tau^- \to e^+e^-\nu_\tau\nu_e\bar{\nu}_\tau\bar{\nu}_e$ or pair production $t\bar{t} \to e^+e^-\nu_e\bar{\nu}_e b\bar{b}$ have negligible contributions in the high-mass region considered for this analysis.

Source	$Z/\gamma^* \to e^+e^-$	Dijet	Diboson	Total SM	Observed
Events	80.0 ± 8.0	28^{+14}_{-17}	6.8 ± 1.4	115^{+16}_{-19}	120

TABLE I: Summary of the expected and observed numbers of dielectron events with $M_{ee} > 200$ GeV/c^2 in 0.45 fb^{-1}. This luminosity value was used to normalize the contributions from all processes with the exception of the dijet background.

A leading-order calculation is used as the starting point to construct the signal and SM Drell-Yan Monte Carlo distributions [19]. A next-to-next-to-leading order mass-dependent $K-$factor [2] is then included, followed by a (M_{ee}, $\cos\theta^*$) parameterization of the CDF detector response [20] to dielectron events. This parameterization is extracted by running the full detector simulation on a large sample of $Z/\gamma^* \to e^+e^-$ events generated with PYTHIA such that the distribution in M_{ee} is roughly uniform between 0.03 and 1.05 TeV/c^2.

For a particular Z' model (denoted by *H1*), we isolate the Z' signal by using two variables: the invariant mass of the electron-positron pair M_{ee} in 10 GeV/c^2 bins, and $\cos\theta^*$ in 0.25 bins. The bidimensional distribution $(M_{ee}, \cos\theta^*)$ of the CDF data is used to test two mutually exclusive hypotheses: 1) the *null* hypothesis (*H0*), where data are described by SM Drell-Yan and background distributions, and 2) the *test* hypothesis (*H1*), where data points are described by the Z' signal and background distributions. A test statistic Q is defined as:

$$Q(\vec{d}) = -2 \cdot \ln \frac{P(\vec{d}\,|H1)}{P(\vec{d}\,|H0)} = \text{const} - 2 \cdot \sum_{i=1}^{N_{bin}} d_i \cdot \ln \frac{\mathcal{N}_i^{H1}}{\mathcal{N}_i^{H0}}$$

where N_{bin} denotes the total number of bins in the $(M_{ee}, \cos\theta^*)$ plane, $\vec{d} = (d_1, d_2, \ldots, d_{N_{bin}})$ is the observed data distribution, while $\mathcal{N}_i^{H1}$ and $\mathcal{N}_i^{H0}$ are the expected numbers of events in bin i in the *H1* or *H0* hypotheses, respectively.

Several sources of systematic uncertainty affect our measurement. First, a relative uncertainty of 10% on the total event rate is incurred primarily due to uncertainties in the luminosity measurement (6%), the dielectron

detector acceptance and electron identification efficiency (5%), and the LO calculation (4%). The second dominating effect is the electron energy scale and resolution uncertainty, which modifies the shape of the M_{ee} and $\cos\theta^*$ distributions. The third source is the uncertainty in the background (particularly dijet) estimations. The dijet prediction uncertainty is extracted from the differences in the fake rate measured in kinematically different jet samples. Finally, the uncertainty related to the choice of the parton distribution functions set (CTEQ6M [21]) is evaluated using the Hessian method advocated in Ref. [22], and found to have a negligible effect on our results.

For each of the Z' models (*H1* test hypotheses) mentioned in the first paragraph, a large number of simulated experiments $\overrightarrow{d}$ are drawn either from the *H1* or the *H0* hypotheses, and the corresponding $Q(\overrightarrow{d})$ values are stored in two separate histograms $f^{H1}(Q)$ and $f^{H0}(Q)$, respectively. The systematic uncertainties are accounted for as described in Ref. [23]. The $f^{H1}(Q)$ and $f^{H0}(Q)$ distributions are integrated in the region $Q > Q_0$, where Q_0 is the value measured using the $\overrightarrow{d}$ distribution of the CDF data. If the ratio of the two integrals is less than 5%, then the *H1* model is excluded at 95% confidence level (C.L.) [23].

The CDF data is found to be consistent with the null (no Z') hypothesis, with a probability $P(\overrightarrow{d}\,|H0)$ greater than the values obtained in 87% of *H0* simulated experiments. Figs. 1 and 2 show good agreement between data and Monte Carlo SM distributions for the M_{ee} and $\cos\theta^*$ distributions. For illustration, Fig. 2 also presents the forward-backward asymmetry A_{FB}^{raw} [14] defined as $(N_+ - N_-)/(N_+ + N_-)$, where N_+ and N_- are the numbers of forward ($\cos\theta^* > 0$) and backward ($\cos\theta^* < 0$) events in the given M_{ee} range. The superscript "raw" is used here to emphasize that no detector acceptance, background subtraction, or efficiency corrections are applied. The A_{FB} plot is a common way of representing the mass dependence of the angular distribution.

The sequential Z'_{SM} boson, which has the same couplings to fermions as the SM Z boson, is excluded by our data up to a mass of 850 GeV/c^2, at 95% C.L. It is noted here that using the dielectron invariant mass alone would require roughly 25% more data for the same Z'_{SM} exclusion. In general, the improvement provided by including the $\cos\theta^*$ spectrum depends strongly on the particular Z' under investigation and the integrated luminosity being analyzed. Other Z' theories include grand unification E_6 models [1, 3, 9], where the E_6 gauge group breaks down as $E_6 \rightarrow \mathrm{SO}(10)\times\mathrm{U}(1)_\psi \rightarrow \mathrm{SU}(5)\times\mathrm{U}(1)_\chi\times\mathrm{U}(1)_\psi$, and the SM gauge structure results from breaking down the SU(5) group. Therefore, an extra Z' will be a combination of the two U(1)'s: $Z_{\theta_{E_6}} = Z_\psi \sin\theta_{E_6} + Z_\chi \cos\theta_{E_6}$. Table II lists the 95% C.L. lower limits on the $M_{Z'}$ for the Z_χ, Z_ψ, Z_η, Z_I, Z_N, and the secluded $Z_{\rm sec}$ E_6 models.

Another class of theories addressing electroweak symmetry breaking and the hierarchy problem are the little Higgs theories [4], where Z'_H bosons are predicted in order to stabilize the Higgs mass against quadratically divergent one-loop corrections. In the minimal model of this type (the littlest Higgs), the Z'_H couples to left-handed fermions only, and these couplings are parameterized as functions of the mixing angle cotangent $\cot\theta_H$ [5]. Our results for $\cot\theta_H = 0.3$, 0.5, 0.7, and 1.0 are shown in Table II, and improve the results reported in [6].

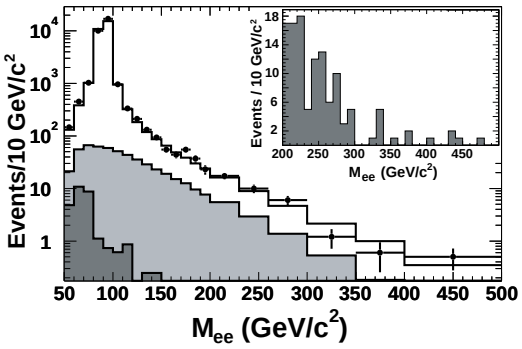

FIG. 1: M_{ee} distribution of the data (points) compared to the prediction for SM Drell-Yan and backgrounds. The individual contributions are stacked as follows: other backgrounds (dark grey), dijet background (light grey), and SM Drell-Yan (open). The inset shows the M_{ee} distribution of high-mass data events using a bin size of 10 GeV/c^2. There are no events in the sample with $M_{ee} > 500$ GeV/c^2.

A recent study reported in [2] defines a more general set of Z' models. This study uses simple constraints such as generation-independent fermion charges and gauge anomaly cancellations to reduce the number of parameters (17) required to define an arbitrary Z' model. Four families of models have been considered, each of them specified by three parameters: the mass $M_{Z'}$, the gauge coupling g_z, and the ratio x of certain $U(1)$ charges. This three-dimensional parameter space is sampled to obtain the exclusion contours shown in Fig. 3. For small $|x|$ and $g_z \leq 0.10$, the exclusion limits are more stringent than the ones derived in Ref. [2] based on the LEP II results [24].

Finally, Z' mass constraints can be derived from searches for contact interactions, if the collider energy is far below the Z' pole [2, 24, 25]. An effective Lagrangian for the $qqee$ contact interaction can be written as: $\sum_q \sum_{i,j=L,R} 4\pi\eta \bar{e}_i\gamma^\mu e_i \bar{q}_j\gamma_\mu q_j/\Lambda^2_{ij}$, where Λ is the scale of the interaction, and $\eta = \pm 1$ determines the interference structure with the Z/γ^* amplitudes [26]. A generation-universal interaction is assumed and lower limits are measured for Λ in six helicity structure scenarios: LL, LR, RL, RR, VV and AA (Table III) [27].

In conclusion, we have searched for Z' decays to e^+e^- pairs in 0.45 fb^{-1} of data accumulated with the CDF II detector. To strengthen this search, the reconstructed

Z' Model	Z_{SM}	Z_χ	Z_ψ	Z_η	Z_I	Z_N	$Z_{\rm sec}$	$Z_H^{0.3}$	$Z_H^{0.5}$	$Z_H^{0.7}$	$Z_H^{1.0}$
Exp. limit (GeV/c^2)	860	735	725	745	650	710	675	625	765	835	910
Obs. limit (GeV/c^2)	850	740	725	745	650	710	680	625	760	830	900

TABLE II: Z' exclusion summary: expected and observed 95% C.L. lower limits on $M_{Z'}$ for the sequential, the canonical E_6, and the littlest Higgs Z' models.

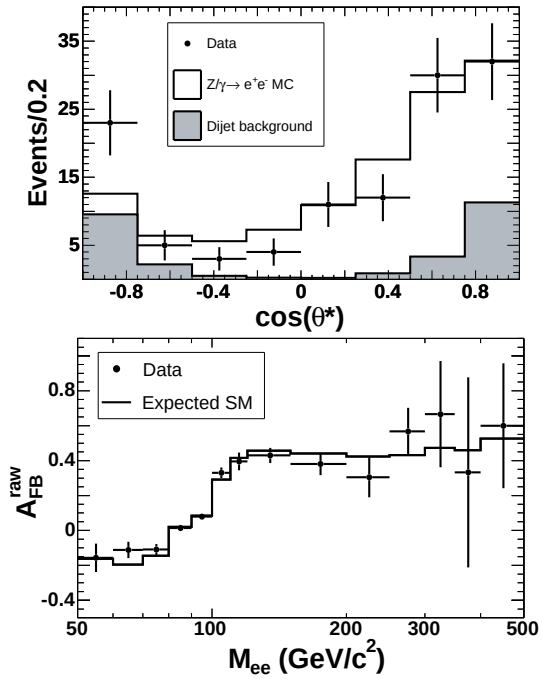

FIG. 2: Top: Distributions of $\cos\theta^*$ for the high mass region $M_{ee} > 200$ GeV/c^2. The points are the data, the open histograms are the predictions from Drell-Yan Monte Carlo simulation, and the shaded histograms are the background predictions. The individual contributions are stacked. Bottom: distributions of the forward-backward asymmetry A_{FB}^{raw} for the data (points) and predicted SM processes (histogram).

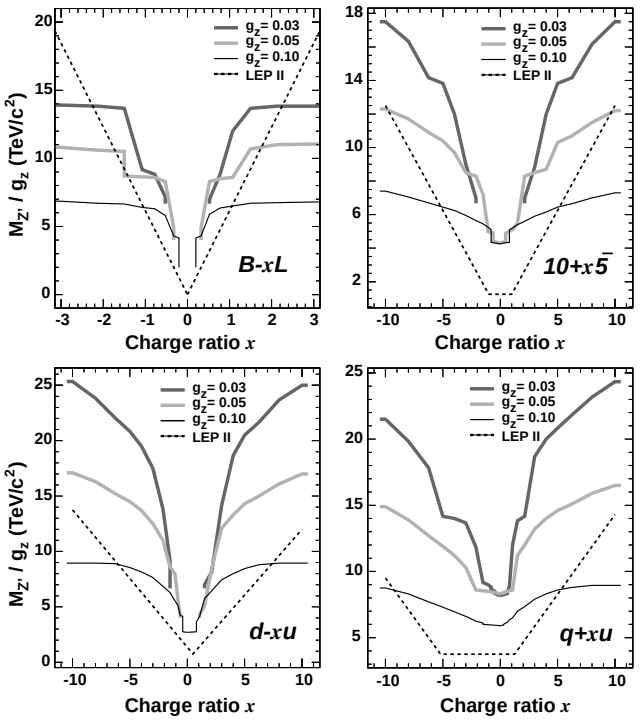

FIG. 3: Exclusion contours for the $B-xL$, $10+x\bar{5}$, $d-xu$, and $q+xu$ Z' families. The dotted lines represent the exclusion boundaries derived in Ref. [2] from the LEP II results [24]. The region below each curve is excluded by our data at 95% C.L. Only models with $M_{Z'}$ >200 GeV/c^2 are tested, which explains the gap at small $|x|$ for some models.

Interaction	LL	LR	RL	RR	VV	AA
Λ_{qe}^+ limit (TeV/c^2)	3.7	4.7	4.5	3.9	5.6	7.8
Λ_{qe}^- limit (TeV/c^2)	5.9	5.5	5.8	5.6	8.7	7.8

TABLE III: 95% C.L. lower limits for the contact interaction mass scales.

dielectron invariant mass M_{ee} spectrum and the angular distribution of the electron pair $\cos\theta^*$ are analyzed simultaneously. This is the first study of this kind at the Tevatron, and it opens up a new avenue for exploring the Z' production in the inverse femtobarn luminosity regime. Many of the Z' models encountered in the literature are surveyed, no significant evidence for signal is found, and 95% C.L. limits are set on these models. Constraints are also placed on contact interaction mass scales far above the Tevatron energy. Finally, exclusion contours for the generic Z' model-lines advocated in Ref. [2] are mapped out. In comparison to the LEP contact interaction Z' search results given in [2], our results exhibit higher sensitivity in the small $|x|$ and small g_z regions.

We thank the Fermilab staff and the technical staffs of the participating institutions for their vital contributions. This work was supported by the U.S. Department of Energy and National Science Foundation; the Italian Istituto Nazionale di Fisica Nucleare; the Ministry of Education, Culture, Sports, Science and Technology of Japan; the Natural Sciences and Engineering Research Council of Canada; the National Science Council of the Republic of China; the Swiss National Science Foundation; the A.P. Sloan Foundation; the Research Corporation; the Bundesministerium für Bildung und Forschung, Germany; the Korean Science and Engineering Foun-

dation and the Korean Research Foundation; the Particle Physics and Astronomy Research Council and the Royal Society, UK; the Russian Foundation for Basic Research; the Comisión Interministerial de Ciencia y Tecnología, Spain; in part by the European Community's Human Potential Programme under contract HPRN-CT-2002-00292; and the Academy of Finland. We thank M. Carena, B. Dobrescu, P. Langacker, H. Logan, and T. Tait for many fruitful discussions.

[1] F. del Aguila, M. Quiros, and F. Zwirner, Nucl. Phys. **B287**, 419 (1987); J. L. Hewett and T. G. Rizzo, Phys. Rept.**183**, 193 (1989).
[2] M. Carena *et al.*, Phys. Rev. D **70**, 093009 (2004).
[3] J. Erler *et al.*, Phys. Rev. D **66**, 015002 (2002); T. Han *et al.*, Phys. Rev. D **70**, 115006 (2004).
[4] N. Arkani-Hamed *et al.*, J. High Energy Phys. 07, 034 (2002).
[5] T. Han *et al.* Phys. Rev. D **67**, 095004 (2003).
[6] A. Abulencia *et al.* (CDF Collaboration), Phys. Rev. Lett. **95**, 252001 (2005).
[7] D. Acosta *et al.* (CDF Collaboration), Phys. Rev. Lett. **95**, 131801 (2005).
[8] J. L. Rosner, Phys. Rev. D **54**, 1078 (1996); T. Affolder *et al.* (CDF Collaboration), Phys. Rev. Lett. **87**, 131802 (2001).
[9] J. L. Rosner, Phys. Rev. D **35**, 2244 (1987).
[10] J. Kang and P. Langacker, Phys. Rev. D **71**, 035014 (2005).
[11] D. Acosta *et al.* (CDF Collaboration), Phys. Rev. D **71**, 032001 (2005); F. Abe *et al.*, Nucl. Instrum. Methods A **271**, 387 (1988); D. Amidei *et al.*, *ibid.* **350**, 73 (1994); P. Azzi *et al.*, *ibid.* **360**, 137 (1995).
[12] In the CDF geometry, θ is the polar angle with respect to the proton beam axis (positive z direction), and ϕ is the azimuthal angle. The pseudorapidity is $\eta = -\ln[\tan(\theta/2)]$. The transverse momentum, p_T, is the component of the momentum projected onto the plane perpendicular to the beam axis. The transverse energy E_T of a shower or calorimeter tower is E $\sin\theta$, where E is the energy deposited.
[13] D. Acosta *et al.* (CDF Collaboration), Phys. Rev. Lett. **94**, 091803 (2005).
[14] D. Acosta *et al.* (CDF Collaboration), Phys. Rev. D **71**, 052002 (2005).
[15] J.C. Collins and D.E. Soper, Phys. Rev. D **16**, 2219 (1977).
[16] T. Sjöstrand *et al.*, Comput. Phys. Commun. **135**, 238 (2001). We use PYTHIA version 6.129a.
[17] U. Baur, T. Han and J. Ohnemus, Phys. Rev. D **48**, 5140 (1993).
[18] J. M. Campbell and R. K. Ellis, Phys. Rev. D **60**, 113006 (1999).
[19] The couplings we use are detailed in C. Ciobanu *et al.*, FERMILAB-FN-0773-E (2005).
[20] GEANT, *"Detector Description and Simulation Tool"*, CERN Program Library Long Writeup W5013 (1993).
[21] H. Lai *et al.*, Phys. Rev. D **51**, 4763 (1995), J. Pumplin *et al.* J. High Energy Phys. 07, 012 (2002).
[22] J. Pumplin *et al.*, Phys.Rev. D **65**, 014013 (2002).
[23] A. L. Read, J. Phys. G: Nucl. Part. Phys. **28**, 2693 (2002); P. Bock *et al.* (the LEP Collaborations), CERN-EP-98-046 (1998) and CERN-EP-2000-055 (2000).
[24] D. Abbaneo *et al.* (the LEP Collaborations) and N. de Groot *et al.* (the SLD Collaboration), CERN-EP/2003-091 (2003).
[25] F. Abe *et al.* (CDF Collaboration), Phys. Rev. Lett. **79**, 2198 (1997).
[26] E. J. Eichten, K. D. Lane, M. E. Peskin, Phys. Rev. Lett. **50**, 811 (1983).
[27] We use: VV(AA)=LL+LR+(−)RL+(−)RR.